Velocity distribution functions of a plasma convecting in the magnetic field of a tangential discontinuity

Gabriel Voitcu[1], Costel Bunescu[1], Marius M. Echim[1,2]

[1]Institute for Space Sciences, Bucharest, Romania

[2]Institut d'Aeronomie Spatiale de Belgique

I. Abstract

A hydrogen plasma is injected into a steady state magnetic field distribution of a 1D tangential discontinuity (TD). It is supposed that the TD is an equilibrium solution for the global plasma flow and field. The moving plasma cloud would be then a perturbation to this equilibrium configuration. This situation is encountered when the magnetopause is a TD and interacts with incoming plasma inhomogeneities/clouds. In our steady state model the magnetic field changes orientation and intensity from $\mathbf{B}_1$ at the "left" hand side of the discontinuity to $\mathbf{B}_2$ at the "right" hand side. The initial velocities of the protons and electrons take values consistent with a velocity distribution function (VDF) described by a displaced Maxwellian. The initial value of the electric field is equal to $\mathbf{E}_1=\mathbf{B}_1\times\mathbf{V}_0$, where $\mathbf{V}_0$ is the the initial bulk velocity of the two populations. The electromagnetic field depends on only one spatial coordinate, x. Two different, prescribed, electric field distributions are tested: (i) a uniform electric field equal everywhere to $\mathbf{E}_1$ and (ii) a non-uniform electric field that is everywhere perpendicular to **B** and has an intensity that satisfies the condition that the electric drift is conserved: $\mathbf{E}\times\mathbf{B}/\mathbf{B}^2$=const. The particles are injected from sources distributed along the x-axis. The particles orbits are integrated numerically. The velocity distribution function is reconstructed by using the Liouville theorem. We compute the VDF of both species inside and outside the discontinuity and illustrate the variations introduced by the non-uniformities of the electromagnetic field. When the electric field is uniform and perpendicular to a unidirectional magnetic field, a broadening of the reconstructed VDF in the perpendicular direction is evidenced when the particle cloud moves in an increasing magnetic field. When the electric field is non-uniform, conserving the zero order drift and remains everywhere perpendicular to **B**, the VDF remains a displaced Maxwellian all along the discontinuity.

II. Numerical method

Equation to solve: the Vlasov equation for the velocity distribution function (VDF) of each component species:

$$\frac{\partial f_1}{\partial t}+\boldsymbol{v}\cdot\frac{\partial f_1}{\partial \boldsymbol{r}}+\frac{q}{m}\left(\boldsymbol{E}+\boldsymbol{v}\times\boldsymbol{B}\right)\cdot\frac{\partial f_1}{\partial \boldsymbol{v}}=0$$

Method to solve: numerical integration of the characteristics (Speiser et al., 1981; Lyons and Speiser, 1982; Williams and Speiser, 1984; Curran et al., 1987; Curran and Goertz, 1989).

Approximation: rarefied and non-diamagnetic plasma cloud. (The self-consistent perturbation of the TD magnetic field due to the incoming VDF, is neglected. Electric and magnetic fields are prescribed) .

Numerical algorithm:
fourth order adaptive Runge-Kutta-Cash-Karp algorithm.

Code: C language, using MPI.
The simulations were done on a small linux cluster of PCs.

III. Simulation setup

Electric and magnetic field distribution

Magnetic field distribution:

$$\boldsymbol{B}(x)=\frac{\boldsymbol{B}_1}{2}erfc\left(\frac{x}{L}\right)+\frac{\boldsymbol{B}_2}{2}\left[2-erfc\left(\frac{x}{L}\right)\right]$$

where $\mathbf{B}_1$, $\mathbf{B}_2$ represent respectively the magnetic field at x=-∞ and x=+∞; L is the scale length of the TD; *erfc* is the complementary error function.

Electric field distribution:

Two stationary **E**-field distributions were tested:

⇨ **Case A**: a uniform electric field given by $\mathbf{E}=\mathbf{B}_1\times\mathbf{V}_0$=const.

⇨ **Case B**: a non-uniform electric field conserving the zero order drift,$\mathbf{U}_E$=const., given by $\mathbf{E}=\mathbf{B}\times\mathbf{U}_E$.

Initial and reconstructed VDF

The particles were injected from sources aligned along x axis, velocity initialization being done according to a displaced Maxwellian distribution:

$$f_{\alpha 1}\left(v_x,v_y,v_z\right)=N_{\alpha 1}\left(\frac{m_\alpha}{2\pi KT_{\alpha 1}}\right)^{\frac{3}{2}}e^{-\frac{m_\alpha\left[(v_x-V_0)^2+v_y^2+v_z^2\right]}{2KT_{\alpha 1}}}$$

The VDF is reconstructed at different moments of time, inside/outside the TD by applying the Liouville theorem that says that along each particle's orbit:

$$df_{\alpha 1}/d\tau=0$$

Thus in any moment later to the injection, when the particle 'a' has the velocity $\mathbf{v}_a=(v_{ax}, v_{ay},v_{az})$, the probability density $P_{va}(v_{ax}, v_{ay},v_{az})$ to have the velocity in $(v_{ax}+dv_x, v_{ay}+dv_y, v_{az}+dv_z)$ is equal to the initial probability density, P_{va0}, that corresponds to the initial velocity of the particle, $\mathbf{v}_0$.

$$P_{va0}(x_0,y_0,z_0,v_{0x},v_{0y},v_{0z}) = P_{va}(x,y,z,v_x,v_y,v_z)$$

We took care that the initial cloud/jet has enough particles such that the velocity space is reasonably sampled (in average we used 2-300000 partic.).

IV. Case A: Uniform electric field

A1. Unidirectional magnetic field with intense gradient

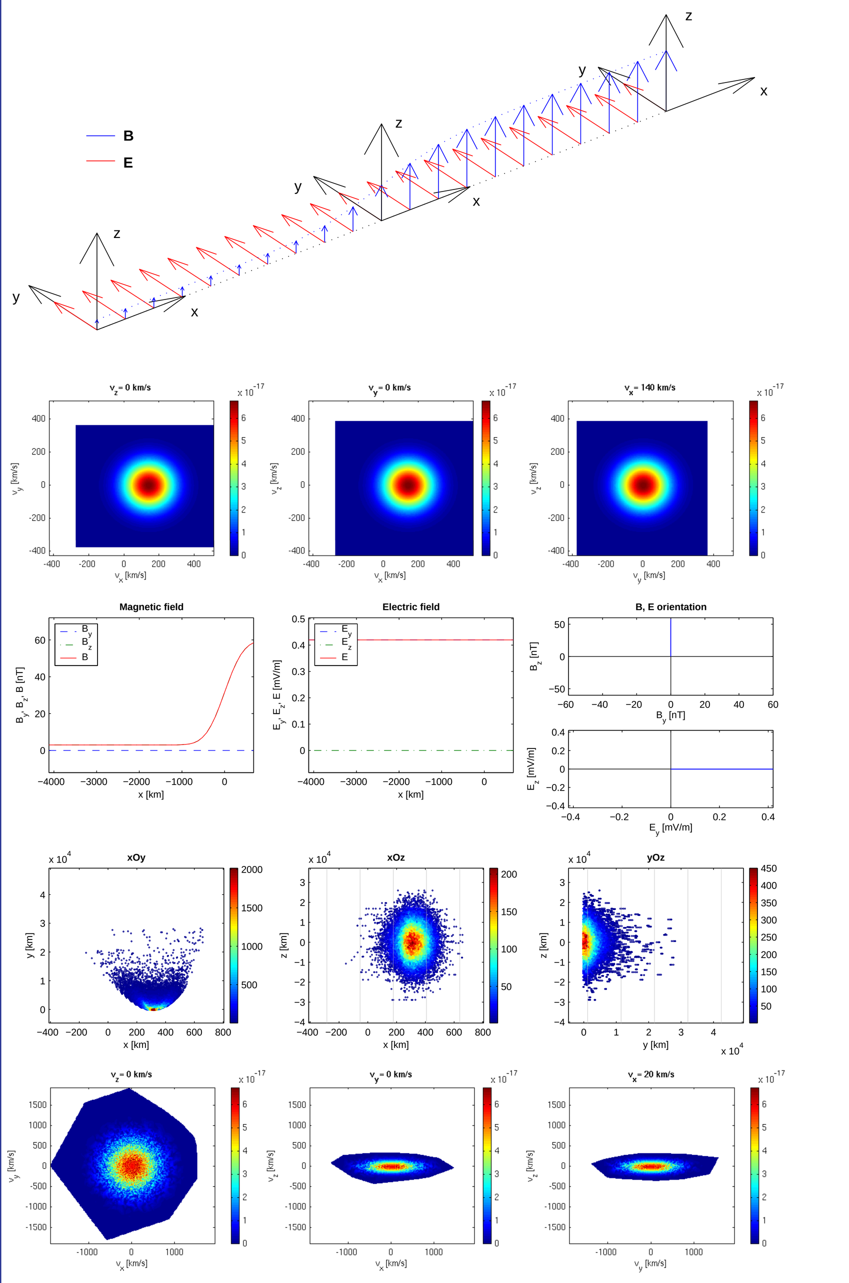

Input parameters

Proton case	Electron case
$\mathbf{B}_1$=(0,0,3)nT, $\mathbf{B}_2$=(0,0,60)nT, L=500km; $\mathbf{E}$=(0,0.42,0)mV/m	
4 sources, 27000 protons/source, x_0=-4120km, dx_0=40km	13 sources, 1000 electrons/source, x_0=-4120km, dx_0=10km
temperature 100eV	temperature 500eV
time of simulation 80s	time of simulation 80s

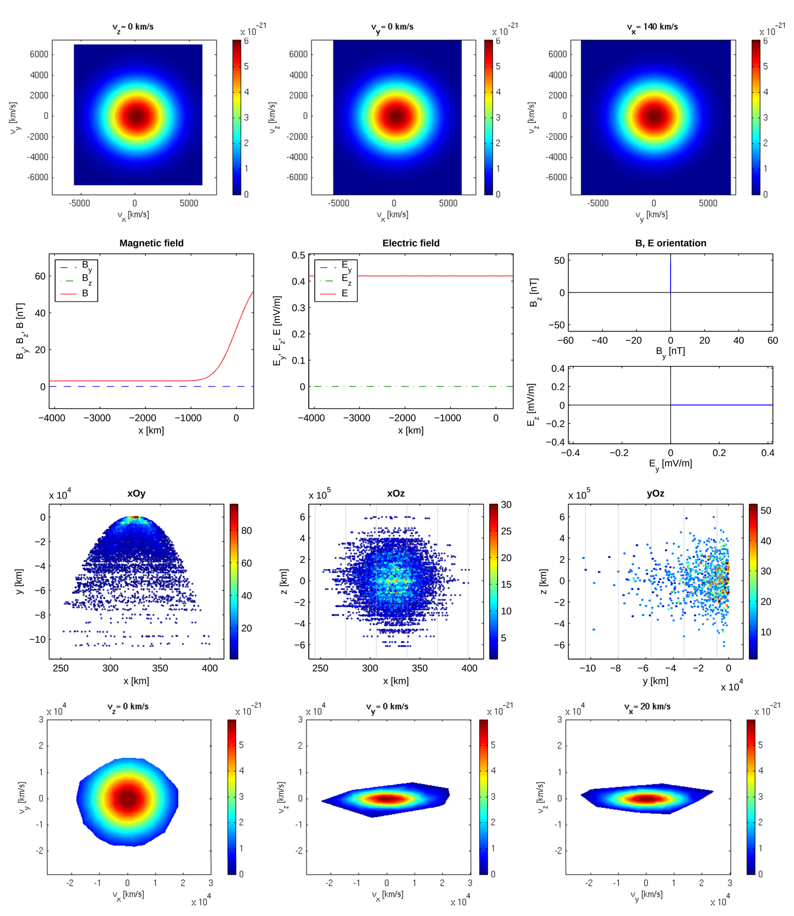

First row: panels show the initial VDF of protons projected in (v_x,v_y), (v_x,v_z), (v_y,v_z) planes of the velocity space.
Second row: first panel shows the magnetic field distribution along the jet's orbit; second panel illustrates the electric field distribution; last panel shows the hodogram of E and B along the jet's path.
Third row: projections in the (xOy), (xOz) and (yOz) of the final positions of all the protons in the jet. The density is color coded.
Fourth row: panels show the final VDF of protons projected in (v_x,v_y), (v_x,v_z), (v_y,v_z) planes of the velocity space.

The format of the data in the panels above is the same as in case A1 - protons (see left for details).

Note the asymmetric deflection of the electron cloud with respect to the proton cloud. This is caused by the charge-dependent grad-**B** drift (see panels 1,3 on the 3rd row).
The perpendicular temperature increases, $T_{perp}>T_0$ (see panel 1 in rows 1 and 4). The parallel temperature, however, remains constant, $T_{parallel} = T_0$ (see panels 2, 3 on rows 1 and 4).

A2. Antiparallel magnetic field

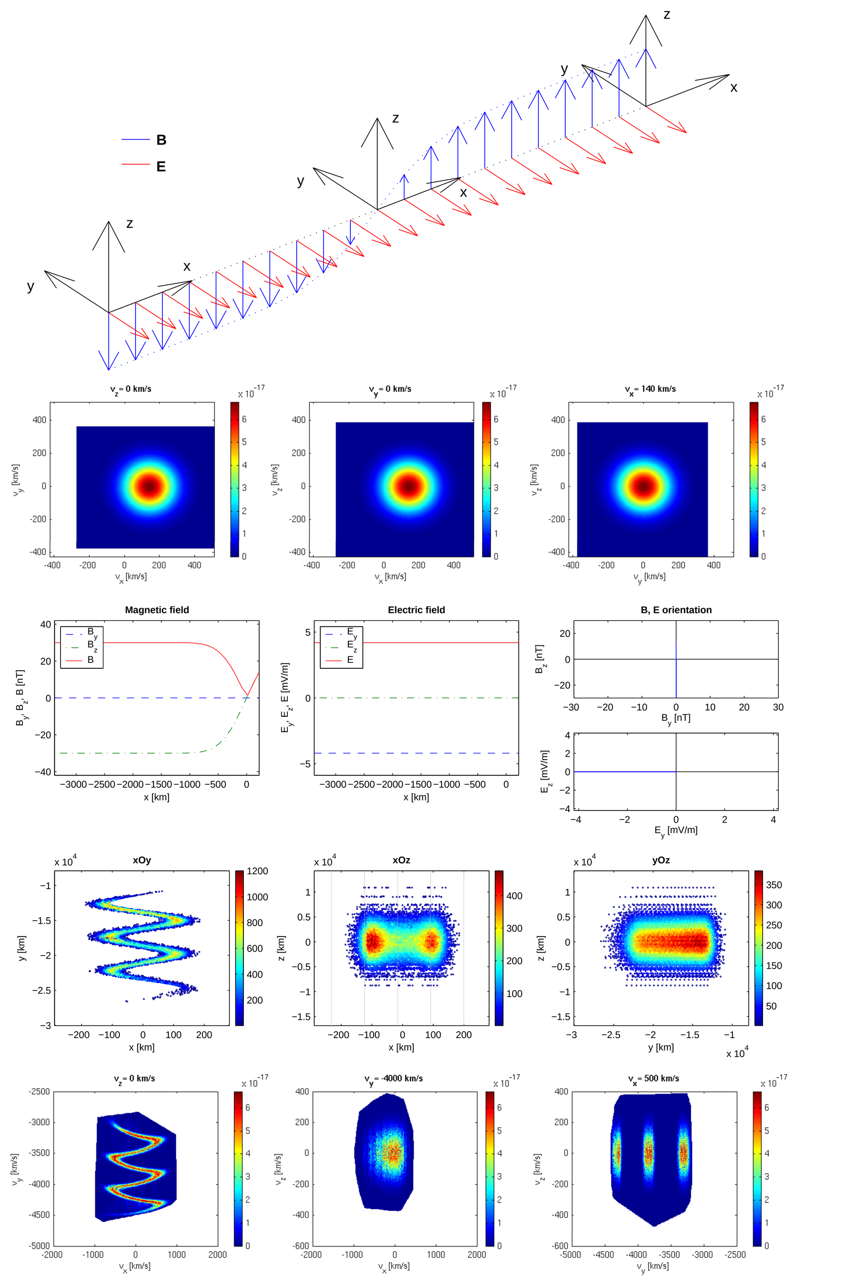

Input parameters

Proton case	Electron case
$\mathbf{B}_1$=(0,0,-30)nT, $\mathbf{B}_2$=(0,0,30)nT, L=500km; $\mathbf{E}$=(0,-4.2,0)mV/m	
20 sources, 27000 protons/source, x_0=-3380km, dx_0=20km	21 sources, 1500 electrons/source, x_0=-3100km, dx_0=5km
temperature 100eV	temperature 500eV
time of simulation 30s	time of simulation 20s

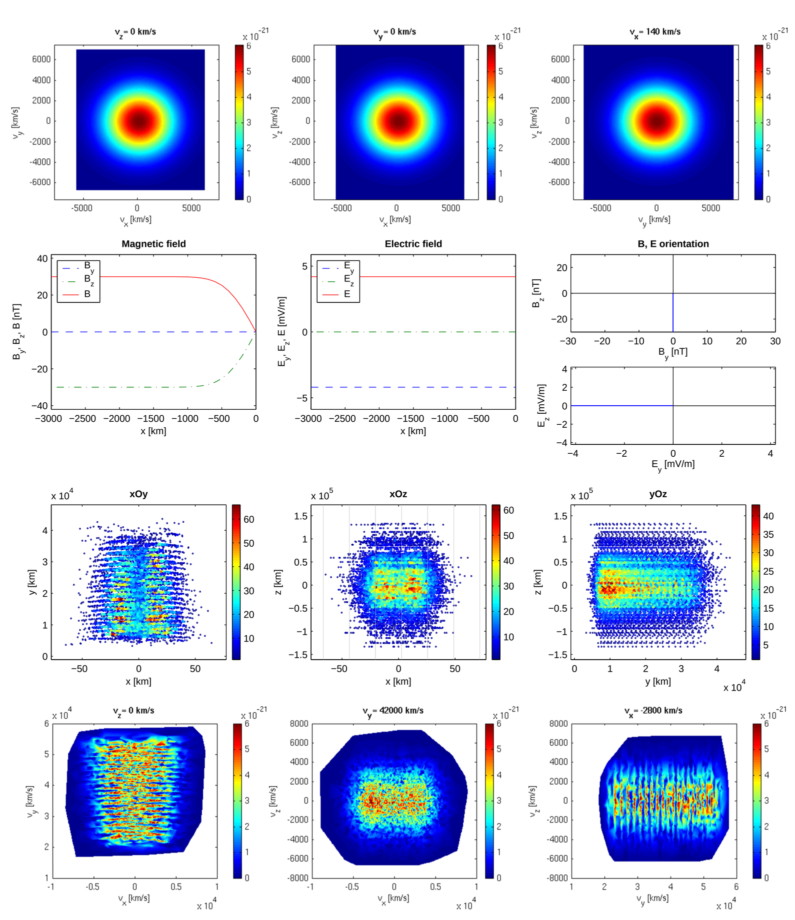

The format of the data in the panels above is the same as in case A1 - protons (see left for details).

The protons are trapped in a sheet of width Wp=400 km, parallel to the TD (panels 1,2 on the 3rd row).

Note the striking iso-morphism between the distribution of proton positions in space and the distribution of their velocities in the velocity space (panel 1 in row 3 and 4). It illustrates the effectiveness of the electrostatic acceleration in the region where **B**=0 and **E**=constant.

The format of the data in the panels above is the same as in case A1 - protons (see left for details).

The electrons are trapped in a sheet of width We=100 km, parallel to the TD and centered in x=0 where **B**=0 and **E**=constant (panels 1,2 on the 3rd row). The maximum velocity of the electrons is roughly 10 times greater than the maximum velocity of the protons.
The structuring, both in space and velocities has a much smaller scale than for the protons. (see panels 1,2 on rows 3 and 4).

IV. Case B: Non-uniform electric field conserving U_E

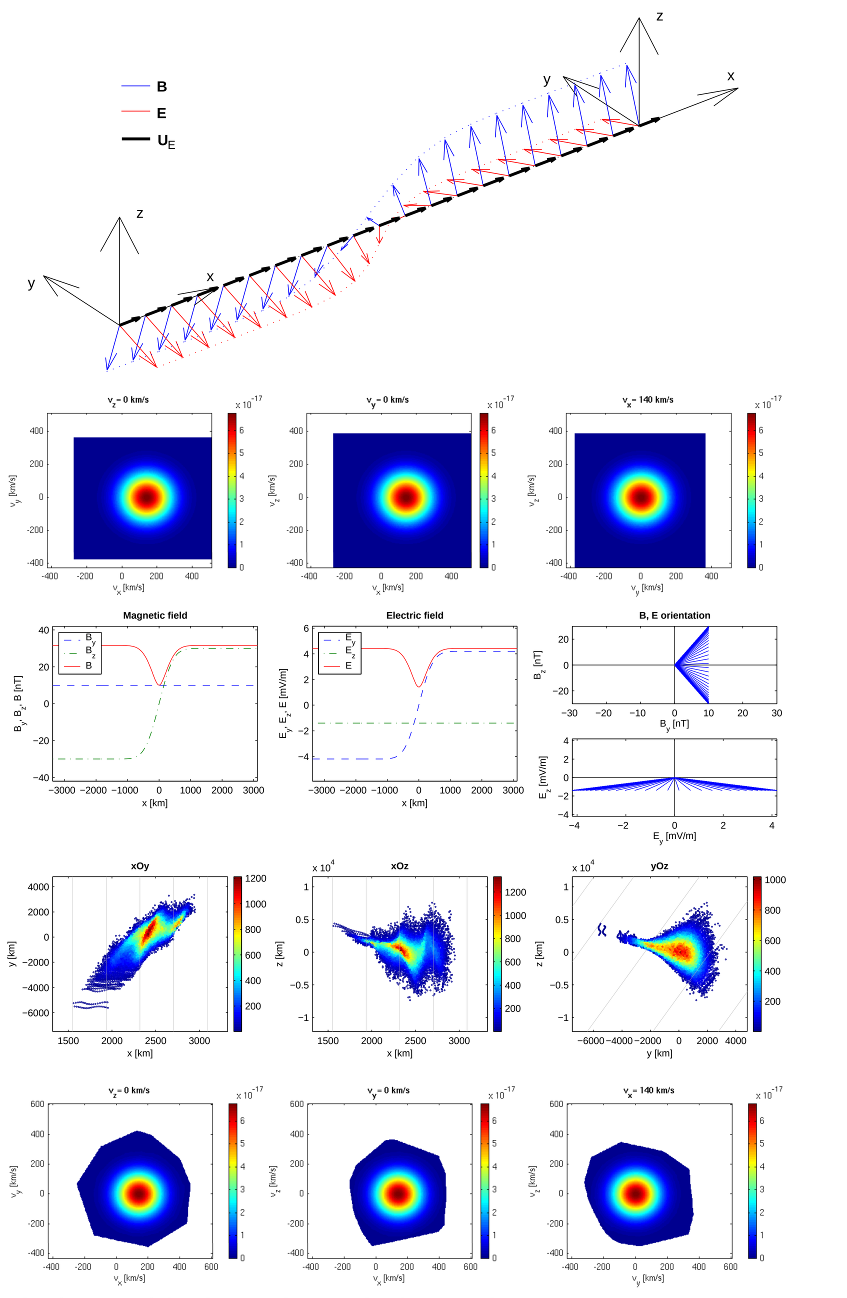

Input parameters

Proton case	Electron case
$\mathbf{B}_1$=(0,10,-30)nT, $\mathbf{B}_2$=(0,10,30)nT, L=500km; $\mathbf{U}_E$=(140,0,0)km/s	
20 sources, 27000 protons/source, x_0=-3380km, dx_0=20km;	77 sources, 1000 electrons/source, x_0=-3380km, dx_0=5km;
temperature 100eV	temperature 500eV
time of simulation 40s	time of simulation 40s

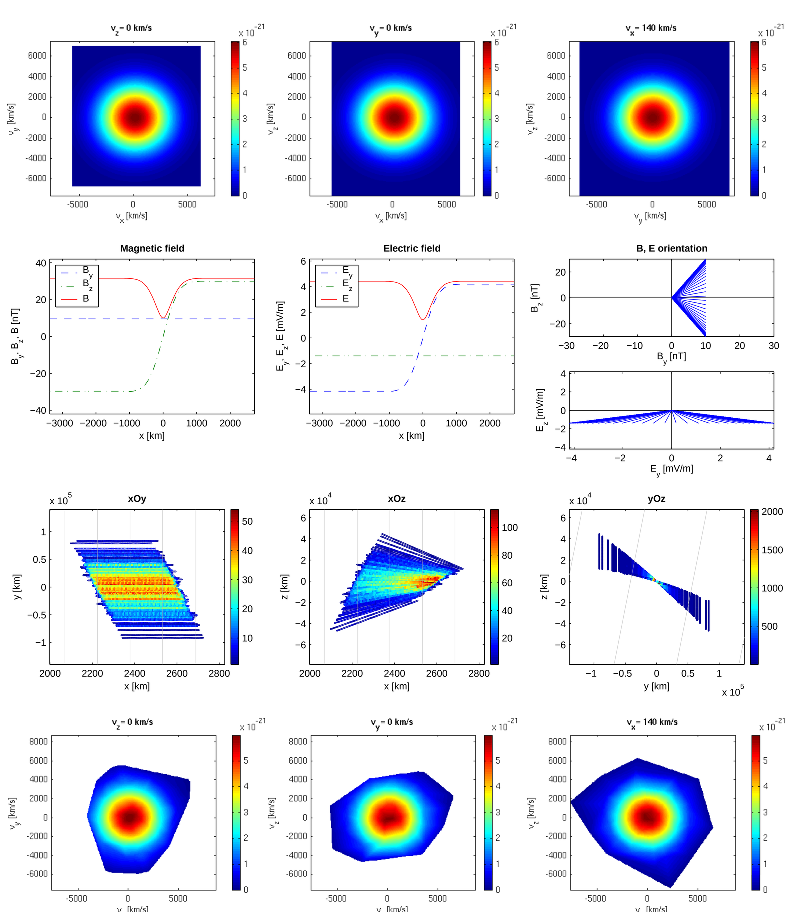

The format of the data in the panels above is the same as in case A1 - protons (see above for details).

The protons penetrate the TD (see panels 1,2 on the 3rd row).

The bulk velocity in the final position of the cloud is equal to the initial velocity, $V_x=V_0$, (panels 1,2 on 4th row).
The shear of **B** inside the TD has deformed the cloud. A wing is formed at the left side (y>0, panels 1,3 on the 3rd row).
The temperature remains isotropic and equal to T_0 (panels 1-3, 4th row).

The format of the data in the panels above is the same as in case A1 - protons (see above for details).

The electrons penetrate along the same distance as the protons (panels 1,2 on the 3rd row).

The electron cloud is much more confined. It has two symmetric wings (panels 1,3 on the 3rd row). Their temperature remains isotropic as for protons (panels 1-3, row 4).

V. Conclusions

- **A1**. The velocity distribution function (VDF) of the electrons and protons of a jet injected normal to a TD is reconstructed using the method of numerical integration of the characteristics of the stationary Vlasov equation.

In the case of an increasing, unidirectional magnetic field the initial VDF of the jet injected perpendicular to **B** is a displaced Maxwellian. It gradually changes to a bi-Maxwellian. This is an effect due the conservation of the total energy and of the magnetic moment. The anisotropy of the resultant VDF depends on the gradient of the magnetic field intensity. The bulk energy of the jet is gradually transformed into gyration energy while the jet moves in the region of increasing field. There is no parallel electric field.

The height of the magnetic barrier determines also the distance over which the jet moves across the non-uniform **B**-field distribution. The reconstructed VDF and the final bulk velocity of the jet illustrate the process of "adiabatic braking" discussed theoretically by Demidenko et al. (1969, 1972) and included in the model of plasma impulsive penetration at the magnetopause by Lemaire (1985).

- **A2**. The VDF of the protons and electrons of a jet injected into an anti-parallel magnetic field distribution and an uniform electric field is highly anisotropic in the velocity and position space. The finite perpendicular electric field accelerates electrostatically the electrons and ions in the region where Bz changes from negative to positive values and **B**=0. There is no parallel electric field.

The jet injected normal to the TD has an initial cylinder-like shape, aligned with the Ox-direction. It is eventually transformed into a current sheet (CS) parallel to the Oy-axis and the TD. The particles are trapped in the current sheet that is centered in x=0 where **B**=0. Within the CS the particles energy is proportional to the distance from the impact point (the point where they entered for the first time the **B**=0 region).

- **B**. If **E** remains everywhere perpendicular to **B**, the VDF of protons and electrons of the jet remains a displaced Maxwellian. The jet penetrates the TD and move across it into the right hand side (that would correspond to the LLBL in the case of a magnetopause crossing). The shear angle of the magnetic field produces a deformation of the shape of the jet, which is more pronounced for the proton population. In this case the variation of the Bz component from negative to positive values does not correspond to acceleration or trapping.

VI. References

[1] M. Echim, Cosmic Research, 40, 534, 2002
[2] M. Echim, J. Lemaire, “Earth's Low Latitude Boundary Layer" AGU Monograph 133, pp. 169-179, American Geophysical Union, 2003.
[3] M. Echim, Ph. D. Thesis, Universite Catholique de Louvain, Belgia, 2004
[4] Speiser, T.W., D.J. Williams, H.A. Garcia, J. Geophys. Res., 86, 723, 1981
[5] Lyons, L.R., Speiser, T.W., J. Geophys. Res., 87, 2276, 1982
[6] Williams, D.J., Speiser, T.W., J. Geophys. Res., 89, 8877, 1984
[7] Curran, D.B., C.K. Goertz, T.A. Whelan Geophys. Res. Lett., 14, 99, 1987
[8] Curran, D.B., C.K. Goertz, J. Geophys. Res., 94, 272, 1989
[9] Adaptive Stepsize Control for Runge-Kutta, pp. 714-722, Numerical Recipes in C
[10] Demidenko, I..I.., Lomino, N.S., Padalka, V.G., Rutkevitch, B.G. And Sinel'nikov, K.D., Soviet Physics-Technical Physics, 14, 16, 1969
[11] Demidenko, I..I.., Lomino and N.S., Padalka, Soviet Physics-Technical Physics, 16, 1096, 1972
[12] Lemaire, J., Journal of Plasma Physics, 33, 425, 1985

"This work was supported by the Romanian Space Agency through contract 72/23.10.2003 (PROSPERO)."